Organic & Biomolecular Chemistry

PAPER

View Article Online
View Journal | View Issue

Cite this: *Org. Biomol. Chem.*, 2014, **12**, 3887

Synthesis and properties of chemiluminescent acridinium ester labels with fluorous tags†

Anand Natrajan,* David Wen and David Sharpe

Received 27th February 2014,
Accepted 28th April 2014

DOI: 10.1039/c4ob00456f

www.rsc.org/obc

Acridinium dimethylphenyl esters are highly sensitive chemiluminescent labels that are used in clinical diagnostics. Light emission from these labels is triggered with alkaline peroxide in the presence of the cationic surfactant cetyltrimethylammonium chloride (CTAC). CTAC compresses emission times of these labels to <5 seconds and also increases overall light yield 3–4 fold. The observed enhancement in acridinium ester chemiluminescence (light yield) is quite sensitive to the polarity of the micellar interface. In the current study, we report the synthesis of new acridinium ester labels with fluorous tags of varying fluorine content and their chemiluminescence in the presence of cationic micelles of CTAC, anionic micelles of sodium perfluorooctanoate (SPFO) as well as mixed micelles of CTAC and SPFO. These studies indicate that in the presence of the mixed micelle system of CTAC and SPFO and at low mole fractions of SPFO, polarity of the mixed micelle interface is lower than that of CTAC leading to a greater enhancement of chemiluminescence for both fluorinated acridinium esters as well as a structurally analogous but non-fluorinated acridinium ester. Chemiluminescence stability of the fluorinated acridinium esters was either comparable to or better than the stability of the non-fluorinated acridinium ester. Non-specific binding to paramagnetic microparticles was higher for fluorinated acridinium esters requiring a surfactant wash to reduce their non-specific binding to the same extent as that observed for the non-fluorinated acridinium ester.

Introduction

Acridinium dimethylphenyl esters[1] (Fig. 1) are highly sensitive and stable chemiluminescent labels that are used in clinical diagnostics in Siemens Healthcare Diagnostics' ADVIA Centaur® systems. These chemiluminescent compounds are used to label both proteins such as antibodies as well as small molecules and the resulting conjugates are used in conjunction with magnetic microparticles in automated immunoassays. A variety of structural modifications can be introduced in the acridinium ring or the phenolic ester leaving group to increase light yield, manipulate emission kinetics, increase aqueous solubility and lower the non-specific binding of the labels.[1]

Light emission from acridinium esters and their conjugates is triggered with alkaline peroxide which adds to C-9 of the acridinium ring (Fig. 2) thereby initiating a series of reactions that ultimately result in the formation of the primary emitter, excited state acridone **VI**.[2] At physiological pH, most acridinium ester labels and their conjugates exist as water-adducts that are commonly referred to pseudobases (**I** in Fig. 2).[1f,g,3] Consequently, an acid pre-treatment step is needed to convert the pseudobase **I** to the acridinium form **II** before the latter can react with peroxide. In practice, at the end of each immunoassay on the ADVIA Centaur® system, light emission is triggered by the sequential addition of 0.3 mL of 0.1 M nitric acid with 0.5% hydrogen peroxide followed by 0.3 mL of 0.25 M NaOH containing 7 mM cetyltrimethylammonium chloride (CTAC).[1d,f] CTAC compresses emission kinetics of the labels from approximately 60 seconds to <5 seconds and increases overall light yield 3–4 fold.[1d,f] The increase in emission kinetics can be attributed to strong hydroperoxide ion binding to the surface of cationic CTAC micelles which increases their local concentration and facilitates formation of the peroxide adduct **III**. CTAC also provides a low polarity environment (alcohol-like) which is conducive to formation of both dioxetane **IV** and dioxetanone **V** precursors to excited state acridone **VI**.[1d,f] Obviously, both these effects also require strong partitioning of the acridinium esters and their conjugates to CTAC micelles which occurs mainly through a combination of hydrophobic and charge interactions.[1f] In our detailed studies we provided evidence that minimally, two acridinium ester

Siemens Healthcare Diagnostics, Advanced Technology and Pre-Development, 333 Coney Street, East Walpole, MA 02032, USA. E-mail: anand.natrajan@siemens.com; Fax: +1-508-660-4591; Tel: +1-508-660-4582

†Electronic supplementary information (ESI) available. See DOI: 10.1039/c4ob00456f

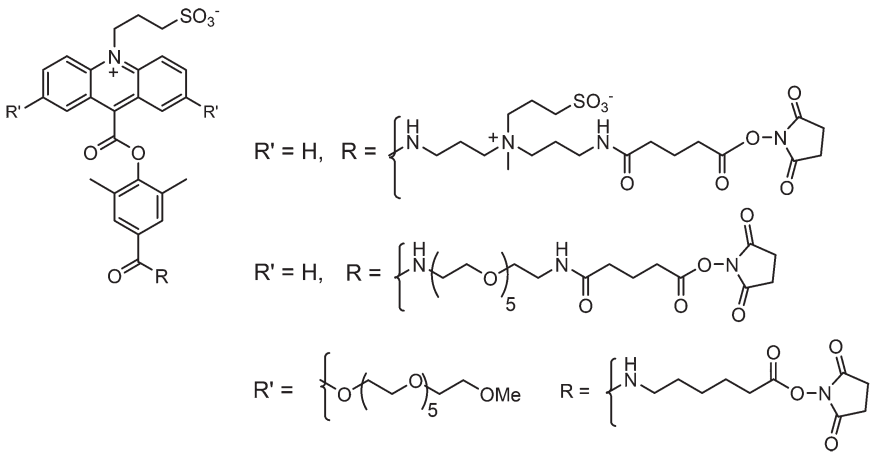

Fig. 1 Structures of chemiluminescent acridinium dimethylphenyl ester labels[1] that are used in automated immunoassays in Siemens Healthcare Diagnostics' ADVIA Centaur® systems.

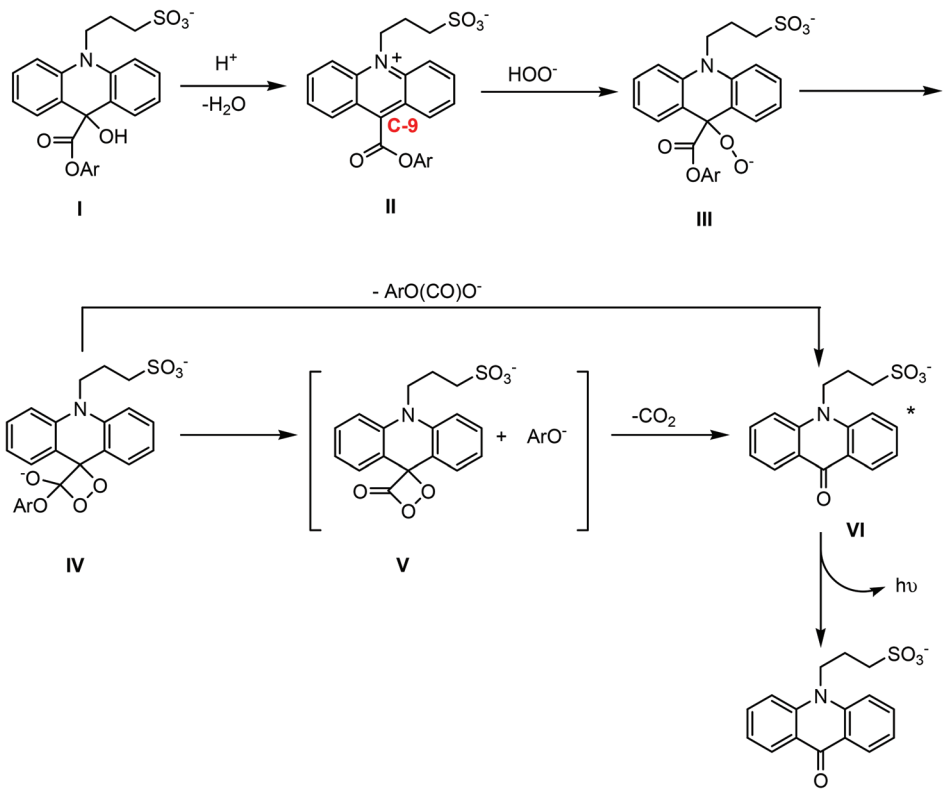

Fig. 2 Simplified reaction pathway of chemiluminescence from *N*-sulfopropyl acridinium esters.[1d,f] Cationic surfactants such as CTAC accelerate conversion of **II** to **III** by increasing the local concentration of hydroperoxide ions. They also facilitate formation of dioxetane **IV** and/or dioxetanone **V** by offering a lower polarity medium for these reactions which involve charge dispersal in their transition states.

intermediates bind with different strengths to CTAC micelles and that micelles affect light emission by two discrete mechanisms.[1d,f]

In immunoassays that use acridinium ester labels (or any other luminescent tag) along with microparticles, optimal assay sensitivity is dependent upon maximizing the specific signal while minimizing non-specific binding. Acridinium esters tend to be hydrophobic and in recent publications,[1] we have outlined strategies to mitigate non-specific binding of these labels to microparticles, without disrupting their binding to CTAC micelles, by incorporating poly(ethylene) glycol (PEG) or zwitterions in these labels. These PEG and

zwitterion containing acridinium esters display excellent aqueous solubility, low non-specific binding and consequently improved sensitivity in immunoassays.[1]

PEG or zwitterion modification of surfaces is also a very useful and widely described strategy to reduce the 'stickiness' of various surfaces to proteins and other macromolecules.[4] More recently, an interesting approach to create protein-resistant surfaces has been described in the literature using fluorination rather than PEG or zwitterion modification.[5] Fluorinated surfaces show low non-specific binding and appear very useful for the construction of protein arrays as well as for the immobilization of molecules containing fluorous tags *via* fluorous (F–F) interactions.[5,6] Fluorous interactions are very specific and have been used in a wide range of applications including fluorous immobilization and extraction,[6,7] fluorous chromatography[8] and numerous other applications. Fluorinated molecules are also selectively solubilized in aggregates of fluorinated surfactants.[9] A recent book edited by Horváth describes some of the more recent applications of fluorous chemistry.[10]

Another vast body of research pertaining to fluorinated materials is in the field of fluorinated surfactants and a comprehensive compilation of research in this area can be found in a book edited by Kissa.[11] We were particularly interested to learn from published reports that the commercially available, perfluorinated anionic surfactant sodium perfluorooctanoate (SPFO) forms mixed micelles with cationic surfactants such as cetyltrimethylammonium bromide (CTAB) and dodecyltrimethylammonium chloride.[12] SPFO and the two cationic surfactants were reported to interact synergistically where the cationic surfactant serves as the solvent for SPFO at low mole fractions of SPFO.[12] Moreover, an investigation of the micellar properties of the mixed micelle system formed by CTAB and SPFO using a fluorescent and an ESR probe indicated a microenvironment with a low dielectric constant, high microviscosity and significant penetration of the SPFO chains in the interior of these mixed micelles.[12] Although these mixed micelle systems have been investigated using these types of spectroscopic techniques, there are few studies on how such mixed micellar systems would impact reaction pathways.

In our previous studies, we observed that acridinium ester chemiluminescence is quite sensitive to the polarity of the micellar interface.[1d,13] Less polar micelles derived from cationic surfactants with large head groups increase the luminescence (light yield) of acridinium esters by facilitating the formation of dioxetane **IV** and dioxetanone **V** (Fig. 2). Based on the above reports on the interaction of SPFO with cationic micelles, we became interested in determining whether fluorous tags incorporated in acridinium esters could be used as a handle to enhance solubilization in both CTAC as well as mixed micelles of CTAC + SPFO (Fig. 3, panel A). Would fluorous chains in acridinium esters increase partitioning into less polar regions of CTAC micelles which would then be reflected by an increase in light yield? We also wanted to investigate how mixed micelles of CTAC + SPFO would affect chemiluminescence from fluorinated acridinium ester labels in comparison to CTAC and SPFO micelles individually, and what could be learnt about the micellar environment of these mixed micelles in relation to the proposed mechanism outlined in Fig. 2? Other specific questions we hoped to address were, how does fluorous content in acridinium esters with, or without charge augmentation (to SPFO) affect chemiluminescence (emission kinetics and enhancement) from mixed micelles of CTAC + SPFO? Finally, we also wanted to evaluate the non-specific binding of the fluorinated acridinium esters to microparticles to determine their relative lipophilicity when compared to a non-fluorinated acridinium ester.

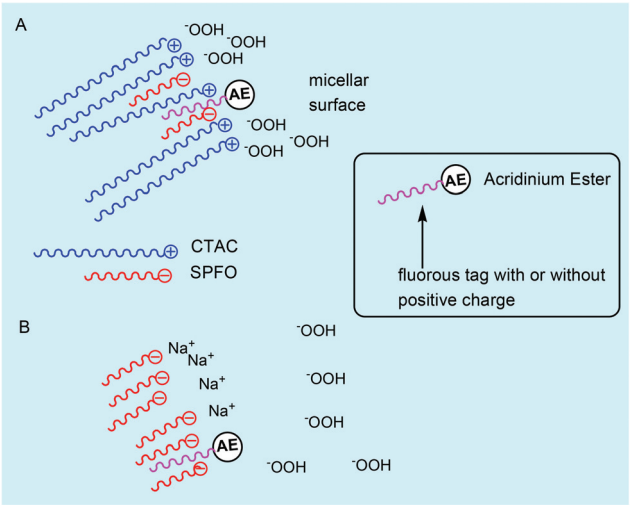

Fig. 3 Panel A: Model for interaction of acridinium esters (AEs) containing fluorous tags with mixed micelles of cetytrimethylammonium chloride (CTAC) and sodium perfluorooctanoate (SPFO). Binding of fluorinated acridinium esters to mixed micelles is through a combination of hydrophobic, charge and fluorous interactions. Only fluorous interactions are shown. Panel B: Model for interaction of acridinium esters (AEs) with fluorous tags with anionic micelles of SPFO. Fluorinated acridinium esters bound to SPFO micelles exhibited a greater inhibition of emission kinetics and loss of light yield with increasing fluorous content.

To answer all these questions, in the present study we report the syntheses and properties of new acridinium ester labels with fluorous tags and varying fluorine content with or without positive charges appended near the fluorous chains (Fig. 4).

Results and discussion

Synthesis of fluorinated acridinium esters and bovine serum albumin (BSA) conjugates

The structures of fluorinated acridinium esters that we elected to synthesize in the present study are illustrated in Fig. 4. Both for ease of synthesis and to ensure strong partitioning of the acridinium ring in these compounds into surfactant aggregates, we decided to incorporate the fluorous chains at C-2 of the acridinium ring. In structures **5a**, **5b** and **5c**, the length of the fluorous 'ponytail' was increased from 9 fluorines in **5a**, to 13 fluorines in **5b** and 17 fluorines in **5c**. For convenience we

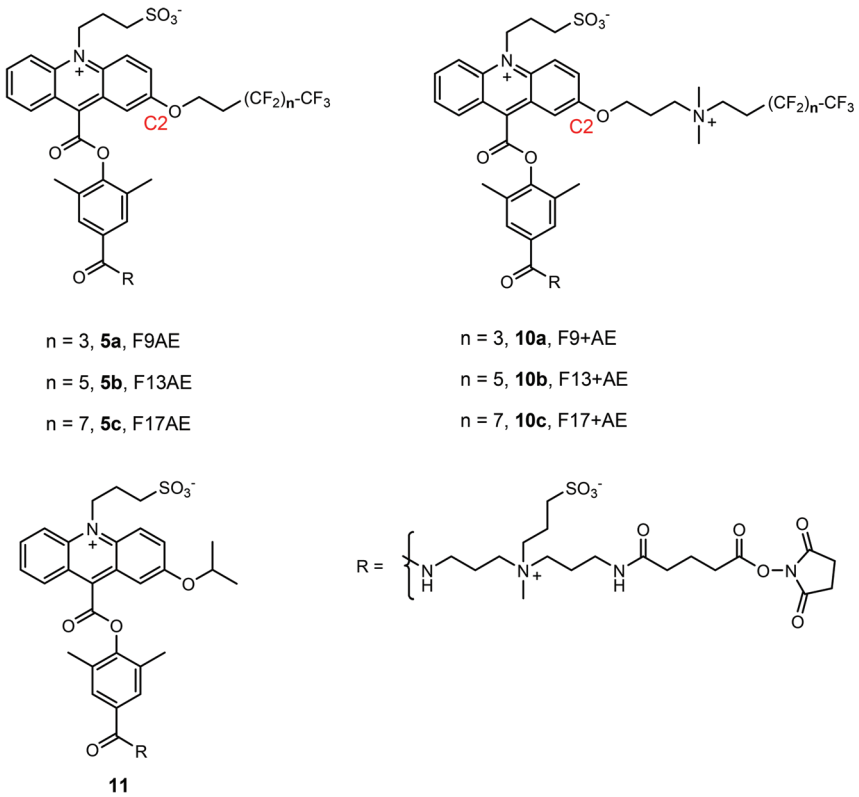

Fig. 4 Structures of fluorinated acridinium esters (F*n*AEs) **5a–5c** and (F*n*+AEs) **10a–10c** synthesized in the current study. AEs **5a**, **5b** and **5c** contain fluorous chains of increasing length and are designated by the number of fluorine atoms (F9AE, F13AE and F17AE). Compounds **10a**, **10b** and **10c** contain a positive charge in addition to fluorous chains of increasing length and are designated by the number of fluorine atoms with a positive charge (F9+AE, F13+AE, F17+AE). Compound **11**,[1f] is an acridinium ester without any fluorines but with the same C-2 alkoxy substitution pattern.

shall henceforth refer to these compounds as F9AE for **5a** (AE = acridinium ester), F13AE for **5b** and F17AE for **5c**. In structures **10a** (9 fluorines), **10b** (13 fluorines) and **10c** (17 fluorines), a positive charge in the form of a quaternary nitrogen was introduced between the acridinium ring and adjacent to the fluorous chains. Using a similar nomenclature, as described for **5a–5c**, compounds **10a**, **10b** and **10c** shall be referred to as F9+AE, F13+AE and F17+AE respectively.

The common synthetic scheme for F9AE, F13AE and F17AE is shown in Fig. 5. Compound **1**, whose synthesis we described previously[1f] was *O*-alkylated at the phenolic group using 1*H*,1*H*,2*H*,2*H*-perfluorohexyl, -perfluorooctyl and -perfluorodecyl triflates to introduce the various fluorous chains in the acridine ring. The triflates were synthesized from the corresponding fluorinated alcohols using a literature procedure.[14] The fluorinated *O*-alkylated products **2a–2c** were then converted to the final targets using chemistry we have described previously.[1f,g] Thus, N-alkylation of **2a–2c** with 1,3-propane sultone in the ionic liquid 1-butyl-3-methylimidazolium hexafluorophosphate [BMIM][PF_6] was followed by acid hydrolysis of the methyl ester to give the acridinium carboxylic acids **3a–3c**. The water soluble zwitterionic linker[1e] **iv** was then introduced in **3a–3c** to give compounds **4a–4c**, which are the amine derivatives of the final targets. Conversion of **4a–4c** to the *N*-hydroxysuccinimide esters (**5a–5c**, F*n*AEs, Fig. 5) was completed by condensation with glutaric anhydride followed by activation of the resulting carboxylic acids.

In a similar vein, the fluorinated acridinium esters F9+AE, F13+AE and F17+AE with a quaternary nitrogen adjacent to the fluorous chains were synthesized using an analogous synthetic scheme as illustrated in Fig. 6. In this case, the starting acridine ester was compound **6** which is accessible by the Mitsunobu reaction between compound **1** and 3-dimethylamino-1-propanol.[1f] N-alkylation of the exocyclic dimethylamino group in compound **6** with the triflates **i–iii** led to exclusive reaction at this nitrogen to give the fluorinated acridine esters **7a–7c** which in turn were converted to the *N*-sulfopropyl acridinium carboxylic acids **8a–8c** by N-alkylation of the acridine nitrogen with 1,3-propane sultone in [BMIM][BF_4] followed by acid hydrolysis of the methyl ester. Completion of the rest of the synthesis was accomplished as described earlier. HPLC traces of all the intermediates and final compounds of Fig. 5 and 6 are shown in the ESI (Fig. S1–S24†). Yields of intermediates and the final products are indicated in Fig. 5 and 6 and were generally good except for some of the F17 compounds.

The fluorous phase is often thought of as a third phase that is distinct from aqueous and hydrocarbon phases.[10] Based on this classification, the fluorinated acridinium esters of the present study (Fig. 4) can be considered to be comprised of three distinct regions: (a) a relatively hydrophobic acridinium

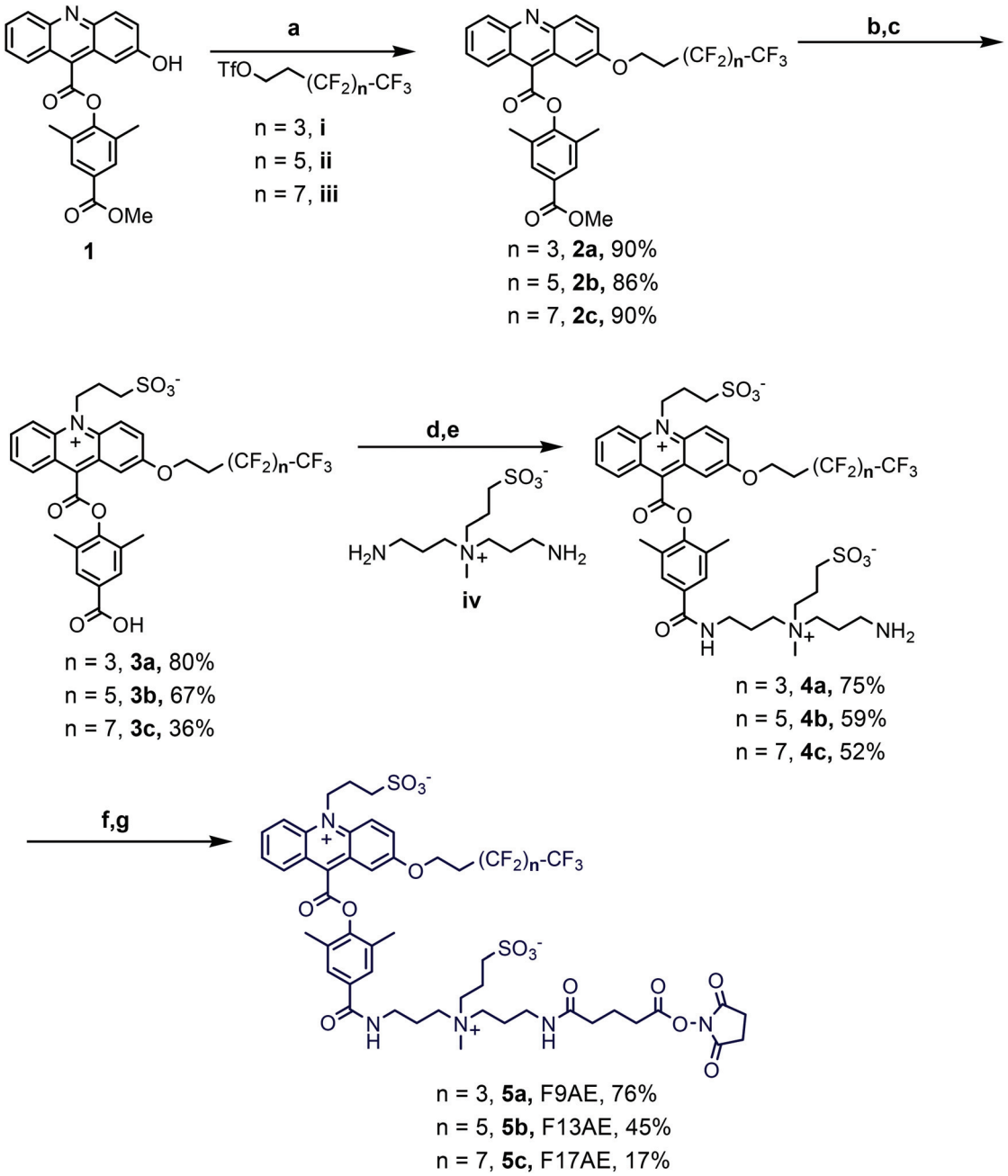

Fig. 5 Synthetic scheme for F*n*AEs **5a–5c**. Reagents: (a) potassium carbonate, MeCN; (b) 1,3-propane sultone, 2,6-di-*tert*-butylpyridine, 1-butyl-3-methylimidazolium hexafluorophosphate [BMIM][PF_6]; (c) 1–2 M HCl–MeCN; (d) *N*,*N*,*N*′,*N*′-tetramethyl-*O*-(*N*-succinimidyl)uronium tetrafluoroborate (TSTU), diisopropylethylamine (DIPEA), DMF; (e) 0.25 M $NaHCO_3$–DMF; (f) glutaric anhydride, DMF–MeOH; (g) TSTU, DIPEA, DMF.

ring and phenolic ester, (b) a highly hydrophilic region containing a sulfobetaine linker that is attached *para* to the phenolic ester and, (c) a fluorous region that is attached to the C-2 of the acridinium ring. In contrast, compound **11** (Fig. 4, reference compound[1f] in the current study) has an electronically similar C-2 alkoxy functional group but only contains hydrophobic and hydrophilic regions.

BSA conjugates of the various acridinium esters of Fig. 4 were prepared using five equivalents input of the *N*-hydroxysuccinimide esters of the labels as described in the ESI† and all gave a similar level of label incorporation of 2–3 labels (Table 1) as determined by mass spectroscopy.

Chemiluminescence measurements

Emission spectra of the fluorinated acridinium esters as well compound **11** were measured using a spectral camera as described in the ESI.† Emission maxima are listed in Table 2 and the complete emission spectra for each compound are shown in the ESI (Fig. S25–S31†). The emission spectra were recorded in a mostly (~90%) aqueous medium and the amine

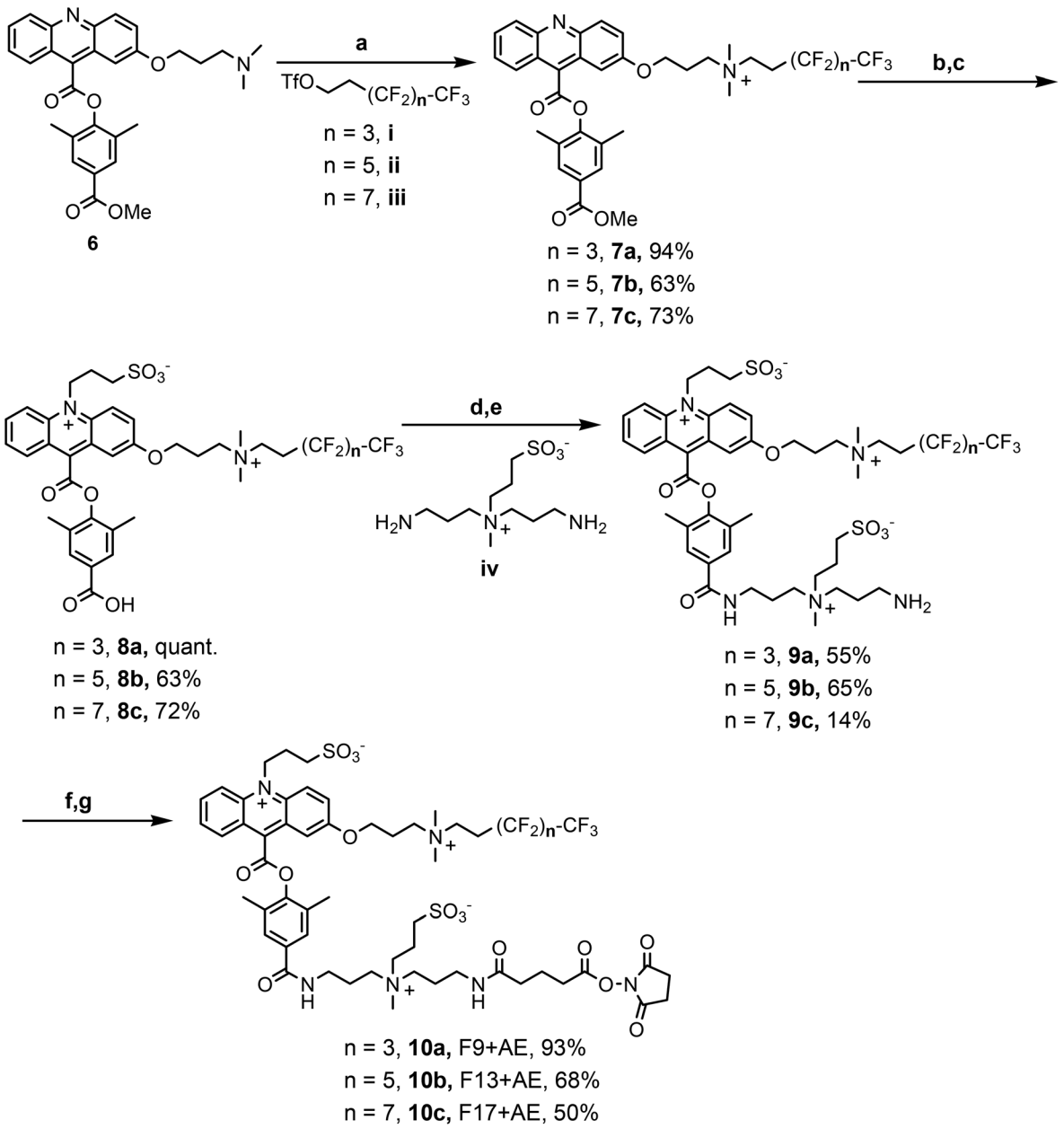

Fig. 6 Synthetic scheme for F*n*+AEs **10a–10c**. Reagents: (a) potassium carbonate, MeCN; (b) 1,3-propane sultone, 2,6-di-*tert*-butylpyridine, 1-butyl-3-methylimidazolium tetrafluoroborate [BMIM][BF_4]; (c) 1–2 M HCl–MeCN; (d) *N*,*N*,*N*′,*N*′-tetramethyl-*O*-(*N*-succinimidyl)uronium tetrafluoroborate (TSTU), diisopropylethylamine (DIPEA), DMF; (e) 0.25 M $NaHCO_3$–DMF; (f) glutaric anhydride, DMF–MeOH; (g) TSTU, DIPEA, DMF.

derivatives of the compounds were used because of their greater aqueous solubility compared to the *N*-hydroxysuccinimide esters. The emission spectra of all the compounds were quite similar and the emission maxima spanned a range of 445–457 nm. The presence of the electron withdrawing fluorous chains closer to the acridinium ring in the F*n*AE series caused a small hypsochromic shift in their emission maxima compared to the F*n*+AE compounds. The reference compound **11**, with a similar C-2 alkoxy group substituent displayed an emission maximum at 454 nm.

Light yield (specific activity) from BSA conjugates of the fluorinated acridinium esters as well as compound **11** are listed in Table 1. For all the acridinium esters, we used BSA conjugates instead of the free labels to ensure complete solubility of the labels in aqueous buffer especially at high dilution that were needed for measurements in the linear range of the photomultiplier tube in the luminometer. (In our previous study we observed that micellar effects on the chemiluminescence of acridinium ester labels are very similar for the free labels as well as the conjugates of the labels.)[1d] The conjugates ~2 mg mL^{-1} were serially diluted into buffer to final concentrations of approximately 0.3 nanomolar (nM) and chemiluminescence was measured using a luminometer from Berthold Technologies. Light emission from a 0.01 mL sample was

Table 1 Acridinium ester incorporation in BSA conjugates measured my mass spectroscopy and specific chemiluminescent activity (SCA) of the labels. Light emission was triggered by the sequential addition of 0.3 mL reagent 1 (0.1 M nitric acid + 0.5% peroxide) followed by 0.3 mL reagent 2 (7 mM CTAC in 0.25 M NaOH). (RLU = relative light unit)

Label	No. of labels by mass spectroscopy	SCA × 10^{-19} RLUs mol^{-1}
11	3	7.0
5a, F9AE	3	8.2
10a, F9+AE	2	11.3
5b, F13AE	2	10.5
10b, F13+AE	2	10.9
5c, F17AE	2	10.8
10c, F17+AE	2	10.4

Table 2 Emission spectra of acridinium esters. Spectra were recorded in >90% aqueous media using a PR-740 spectroradiometer (camera) from Photo Research Inc. Bandwidth slit: 2 nm; aperture: 2 degrees; exposure time: 5000 ms. The amine intermediates were used for these measurements

Compound (amine intermediate)	Emission maximum (nm)
Amine intermediate[1f] of **11**	454
4a, F9AE	446
9a, F9+AE	457
4b, F13AE	445
9b, F13+AE	453
4c, F17AE	445
9c, F17+AE	453

initiated by the sequential addition of 0.3 mL of 0.1 M nitric acid with 0.5% hydrogen peroxide (reagent 1) followed by the addition of 0.25 M sodium hydroxide (reagent 2) containing 7 mM of the cationic surfactant CTAC. Light was measured for 20 seconds integrated at 0.1 s intervals (additional details can be found in the ESI†). The output of the instrument was expressed as Relative Light Units (RLUs). As can be noted from Table 1, the specific chemiluminescent activities, expressed as RLUs per mole, of the fluorinated labels were either comparable or slightly higher compared to that of the non-fluorinated reference compound **11**. The observed small increases in overall light yield increased with increasing fluorous content of the labels. Because all labels have the same C-2 alkoxy substitution pattern which is the main determinant of light yield,[1c,f] the results in Table 1 are expected. Moreover, these results also indicate that the fluorinated acridinium esters can partition strongly into micelles of a non-fluorinated cationic surfactant through a combination of hydrophobic and charge interactions[1f] in a similar manner to **11**.

We then investigated the properties of the mixed micelle system of CTAC and SPFO on acridinium ester chemiluminescence (both light yield and emission kinetics), at different mole fractions of CTAC and SPFO as indicated in Tables 3 and 4. Specifically, CTAC : SPFO ratios were varied from 10 : 1, 5 : 1, 3.3 : 1 and 2.5 : 1. At all ratios of CTAC : SPFO, because CTAC is in excess, the overall charge of the mixed micelle is expected to be positive. Both surfactants were dissolved in 0.25 M sodium hydroxide (reagent 2) and reagent 1 was unchanged in these experiments. No surfactant in 0.25 M sodium hydroxide was used for the control experiment. Besides the CTAC–SPFO mixed micellar system, the effect of aggregates of the individual surfactants CTAC (described above) and SPFO were also investigated. SPFO was used at twice its reported critical micelle concentration.[15]

The effect of the different micellar systems on emission kinetics of the BSA conjugates of the various fluorinated acridinium esters and compound **11** are listed in Table 3 and the complete emission profiles are shown in Fig. S32–S39 (ESI†). The values in Table 3 reflect the time needed (in seconds) for ≥95% emission. For the cationic micellar systems (CTAC and CTAC + SPFO mixtures) where fast light emission was observed, light emission was measured for a total period of 20 seconds integrated at 0.1 second intervals. Light emission was significantly slower in the absence of surfactant and in the presence of anionic micelles of SPFO and in these two cases, light emission was measured for a total period of 120 seconds integrated at 0.5 second intervals.

From the data in Table 3, in the absence of any surfactant, light emission from the conjugates of the different labels was observed to be quite slow with some intrinsic differences between the different labels. In particular, increasing the bulk of the C-2 substituent had an accelerative effect on emission kinetics. For example whereas the time for ≥95% emission was 71 seconds for **11** with a C-2 isopropoxy group, these emission times were compressed to 48.5, 32.5 and 29 seconds for F9AE, F13AE and F17AE respectively. Similarly, emission times decreased from 72, 53.5 and 38 seconds with increasing chain length for F9+AE, F13+AE and F17+AE respectively. The latter compounds with a positive charge near the fluorous chains were observed to be slower emitters. Light emission from acridinium esters is initiated by the addition of hydroperoxide ions at C-9 (Fig. 2) and a remote C-2 functional group is unlikely to influence this reaction. It is possible that an increase in size of the C-2 substituent facilitates faster decomposition of the dioxetane **IV** or dioxetanone **V** precursors presumably because of relief of steric congestion in these reactive intermediates. As to what role a remote positive charge may play in this process is unclear at present.

In mixtures of CTAC and SPFO, at the ratios we examined, overall micellar charge is positive and consequently, light emission from all acridinium ester conjugates was very rapid with emission times of ~2 seconds. Emission times increased marginally as overall positive charge in the mixed micellar system was attenuated by increasing SPFO concentration. Nevertheless this effect was quite small as indicated by the data in Table 3. Clear evidence for fluorous interactions between SPFO and the fluorinated acridinium esters were noticed when emission times were measured in pure anionic micelles of SPFO. For example, whereas the conjugate of non-fluorinated acridinium ester **11** showed similar emission times in the absence of surfactant and SPFO (71 seconds *versus*

Table 3 Time (seconds) for ≥95% total light emission for BSA conjugates of acridinium esters (average of triplicate measurements). Light emission was triggered by the sequential addition of 0.3 mL reagent 1 (0.1 M nitric acid + 0.5% peroxide) followed by 0.3 mL of 0.25 M NaOH containing CTAC (7 mM) or CTAC–SPFO mixtures as indicated. No surfactant in 0.25 M NaOH was the control experiment

Reagent 2	**11**	**5a**, F9AE	**10a**, F9+AE	**5b**, F13AE	**10b**, F13+AE	**5c**, F17AE	**10c**, F17+AE
No CTAC	71.0	48.5	72	32.5	53.5	29	38.0
75 mM SPFO	*79.5*	*79.0*	*78*	*70*	*57*	*74*	*51.5*
CTAC	1.5	1.2	1.0	1.4	0.8	1.3	0.8
CTAC : SPFO, 10 : 1	2.0	1.7	1.5	1.6	1.0	1.6	1.2
CTAC : SPFO, 5 : 1	2.3	1.8	1.8	1.9	1.1	2.0	1.2
CTAC : SPFO, 3.3 : 1	2.0	1.9	1.8	1.8	1.1	1.7	1.1
CTAC : SPFO, 2.5 : 1	2.1	1.9	2.1	2.0	1.4	1.9	1.2

Table 4 Observed relative change in light output of BSA conjugates of acridinium esters (average of triplicate measurements). Light emission was triggered by the sequential addition of 0.3 mL reagent 1 (0.1 M nitric acid + 0.5% peroxide) followed by 0.3 mL of 0.25 M NaOH containing CTAC (7 mM) or CTAC–SPFO mixtures as indicated. No surfactant in 0.25 M NaOH was the control experiment. Observed RLUs in the absence of any surfactant were normalized to one for each label. Maximum observed enhancement values are indicated in bold

Reagent	**11**	**5a**, F9AE	**10a**, F9+AE	**5b**, F13AE	**10b**, F13+AE	**5c**, F17AE	**10c**, F17+AE
No CTAC	1.0	1.0	1.0	1.0	1.0	1.0	1.0
75 mM SPFO	*0.8*	*0.6*	*1.0*	*0.6*	*0.9*	*0.4*	*0.7*
CTAC	5.1	5.3	4.1	4.5	3.4	3.9	2.9
CTAC : SPFO, 10 : 1	5.3	**5.7**	**4.4**	**5.1**	3.7	**4.3**	**3.3**
CTAC : SPFO, 5 : 1	**5.5**	**5.7**	4.3	**5.1**	**3.8**	**4.3**	**3.3**
CTAC : SPFO, 3.3 : 1	5.1	5.4	4.1	5.0	3.6	4.1	3.1
CTAC : SPFO, 2.5 : 1	5.1	5.3	3.7	5.0	3.6	3.9	3.1

79.5 seconds respectively), the fluorinated acridinium esters showed strong inhibition of emission kinetics which increased with increasing fluorous content. Emission times for F9AE, F13AE and F17AE increased from 48.5, 32.5 and 29 seconds respectively in the absence of surfactant to 79, 70 and 74 seconds respectively in the presence of SPFO. Increasing fluorous content in these acridinium esters leads to greater partitioning from bulk medium into fluorinated micelles of SPFO which repel hydroperoxide ions and inhibit emission kinetics. The inhibition in emission kinetics is also clearly evident from a comparison of the emission profiles for the various conjugates in the absence of surfactant and in the presence of SPFO micelles as illustrated in Fig. S39 (ESI†). Interestingly, the compounds F9+AE, F17+AE and F17+AE which were designed to interact with SPFO micelles both by fluorous and charge interactions, showed a more attenuated inhibition of emission kinetics with emission times of 72, 53.5 and 38 seconds respectively in the absence of surfactant, to 78, 57 and 51.5 seconds respectively in the presence of SPFO for ≥95% emission. We conclude from these observations that partitioning of these fluorinated acridinium ester substrates into SPFO micelles is poorer which suggests an absence of any attractive charge interaction between the anionic head group of SPFO and the quaternary nitrogen in these compounds. Increased aqueous solubility of these charged labels may also play a role in poorer partitioning into SPFO micelles.

Micelles also strongly influence light yield from acridinium esters and in Table 4 we have summarized the effect the mixed micellar system of CTAC and SPFO on light yields and have compared it to light yields observed in the absence of surfactant and in the presence of micelles of the individual surfactants CTAC and SPFO. To enable easy comparisons, we have normalized the light yield in the absence of surfactant to one for all acridinium ester conjugates. Inspection of the data in Table 4 indicates that in the mixed micellar system of CTAC and SPFO, light yield is slightly enhanced, compared to CTAC alone, for all acridinium ester conjugates especially at CTAC : SPFO ratios of 10 : 1 and 5 : 1. The conjugate of compound **11** which contains no fluorines also showed enhanced light yield in mixed micelles of CTAC : SPFO at low mole fractions of SPFO. These results indicate that at CTAC : SPFO ratios of 10 : 1 and 5 : 1, the polarity of the mixed micelles is lower than that of CTAC. The observed enhancements in the mixed micellar system at these ratios of CTAC and SPFO are comparable to what we observed previously in less polar aggregates of cationic surfactants with large head groups such as cetyltripropylammonium chloride.[1d] The conjugates of the fluorinated acridinium esters showed a similar trend and the magnitude of the observed enhancement actually decreased slightly with increasing fluorous content for both series of acridinium esters. These observations coupled with the data in Table 1 suggest that the fluorous chains in the fluorinated acridinium esters do not enable partitioning into less polar regions of micelles of either CTAC or CTAC + SPFO.

As SPFO concentration increased, light output was observed to decrease back to the levels of enhancement seen with micelles of pure CTAC. At higher mole fractions of SPFO, partial separation of the CTAC and SPFO phases may occur similar to what has been reported in other mixed micelle systems[16] which could explain the drop in light enhancement although the emission kinetics data (Table 3) indicate that phase separation may not be occurring. A more reasonable

explanation is that at higher concentrations of SPFO, polarity of the mixed micelle is higher and similar to that of CTAC. Table 4 also indicates that in anionic micelles of SPFO, light output is suppressed and the magnitude of this inhibition increased with increasing fluorous content of the acridinium esters F9AE, F13AE and F17AE where observed light yields were 0.6, 0.6 and 0.4 respectively compared to the no surfactant control experiment. These results parallel the strong inhibition in emission kinetics that was observed with these compounds in SPFO micelles (Table 3). Inhibition of light output presumably results from unfavorable electrostatic interactions between the anionic head group of SPFO and negatively charged dioxetane intermediates (**IV** in Fig. 2) that are precursors to excited state acridone. The F*n*+AE series of fluorinated acridinium esters exhibited less severe inhibition of emission kinetics and their light yields were also less affected by anionic micelles of SPFO.

Non-specific binding and chemiluminescence stability

Finally, we examined chemiluminescence stability and non-specific binding of the BSA conjugates of the fluorinated acridinium esters (Fig. 7 and Table 5). Stability is essential for long term storage of reagents and in this regard, the fluorinated acridinium ester labels exhibited stability which was comparable to the reference compound **11**. Under refrigeration at 4 °C, no loss of chemiluminescence occurred whereas at 37 °C, chemiluminescence stability increased with increasing fluorous content which was more clearly evident for the F*n*AE series. The F*n*AE series of compounds exhibited better stability than the F*n*+AE series as can be noted from Fig. 7.

Acridinium dimethylphenyl ester labels are used in conjunction with magnetic microparticles in automated immunoassays in Siemens Healthcare Diagnostics' ADVIA Centaur® systems. Assay sensitivity is a function of both light output of the label and the background signal caused by non-specific binding of the label. We evaluated the non-specific binding of the BSA conjugates of the various fluorinated acridinium ester labels to paramagnetic particles (PMPs) using the non-fluorinated acridinium ester **11** as the reference compound (Table 5). The PMPs used for measurement of non-specific binding were, 1–10 micron-sized iron(III) oxide particles, coated with an anti-fluorescein antibody on the amino-silanized particle surface using commonly used glutaraldehyde coupling chemistry. The particles were mixed with solutions of the acridinium ester-labeled conjugates and were then magnetically separated. They were then washed twice using three different wash solutions: (a) phosphate buffer, pH 7.2, (b) the non-ionic surfactant Tween-20 at a concentration of 0.8 mM in phosphate buffer, and (c) a combination of 0.8 mM Tween-20 with 50 mM SPFO in phosphate buffer. (The cationic surfactant CTAC resulted in particle loss during the magnetic separation step so could not be evaluated as a wash detergent.) The chemiluminescence associated with the particles was then measured. The ratio of this chemiluminescence value in comparison to the total chemiluminescence input is referred to fractional non-specific binding (FNSB) and is a reflection of the resistance of the conjugate towards non-specific adsorption to the microparticles. The results of these measurements are tabulated in Table 5 and details are described in the ESI.†

Compared to the non-fluorinated reference compound **11**, all conjugates of the fluorinated acridinium esters showed significantly higher FNSB when the PMPs were washed only with buffer strongly suggesting that the acridinium rings in these compounds are much more hydrophobic than that of **11** (Table 5). This non-specific binding was exacerbated with increasing fluorous content and the addition of a positive

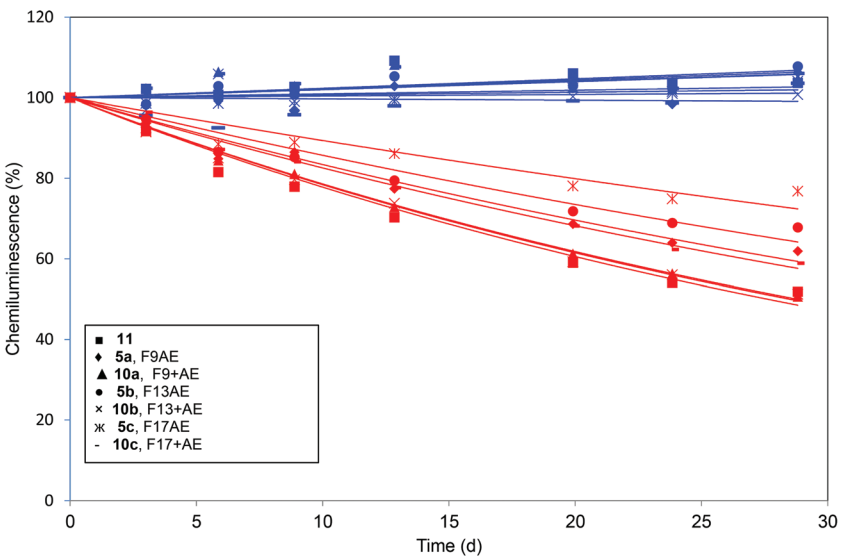

Fig. 7 Chemiluminescence stability of BSA conjugates of acridinium esters at 4 °C (blue lines) and 37 °C (red lines). BSA conjugates of the various acridinium esters were stored in buffer at pH 7.4 either at 4 °C or 37 °C and residual chemiluminescence was measured as a function of time. There was no loss of chemiluminescence at 4 °C. At 37 °C, stability of the fluorinated acridinium ester labels was comparable to the reference compound **11** with slightly enhanced stability with increasing fluorous content which was more evident for the F*n*AE series.

Table 5 Fractional non-specific binding (FNSB) of BSA conjugates of fluorinated acridinium esters and the non-fluorinated acridinium ester **11** to paramagnetic microparticles (PMPs) using three different wash protocols. The fluorinated acridinium esters were observed to be more lipophilic and exhibited higher non-specific binding when the PMPs were washed with only buffer. The non-ionic detergent Tween-20 was effective in reducing the non-specific binding of the fluorinated acridinium esters with lower fluorous content. The addition of SPFO in the wash solution did not reduce non-specific binding any further

	FNSB after wash			Relative FNSB		
Conjugate	Phosphate buffer, pH 7.2	Phosphate buffer + 0.8 mM Tween-20	Phosphate buffer + 0.8 mM Tween-20 + 50 mM SPFO	Phosphate buffer, pH 7.2	Phosphate buffer + 0.8 mM Tween-20	Phosphate buffer + 0.8 mM Tween-20 + 50 mM SPFO
11	3.3×10^{-5}	4.7×10^{-5}	3.8×10^{-5}	1.0	1.4	1.1
5a, F9AE	2.1×10^{-4}	3.4×10^{-5}	3.5×10^{-5}	1.0	0.2	0.2
10a, F9+AE	2.2×10^{-4}	6.8×10^{-5}	7.8×10^{-5}	1.0	0.3	0.4
5b, F13AE	2.1×10^{-4}	4.6×10^{-5}	4.0×10^{-5}	1.0	0.2	0.2
10b, F13+AE	6.6×10^{-4}	3.9×10^{-4}	4.3×10^{-4}	1.0	0.6	0.7
5c, F17AE	3.6×10^{-4}	9.4×10^{-5}	1.1×10^{-4}	1.0	0.3	0.3
10c, F17+AE	5.4×10^{-4}	1.4×10^{-4}	1.5×10^{-4}	1.0	0.3	0.3

charge in the F*n*+AE series of compounds. However, when the non-ionic detergent Tween-20 was used in buffer to wash the particles, the FNSB values of the fluorinated acridinium esters, especially those with lower fluorous content and no positive charge (F9AE and F13AE), were effectively reduced down to the same FNSB value observed for non-fluorinated **11**. Interestingly, Tween-20 was no more effective than plain buffer as a wash solution for **11** which indicates that overall, **11** is a relatively hydrophilic compound. Thus from Table 5, when the observed FNSB values of the various acridinium esters using a buffer wash are normalized to one, a significantly greater drop in the relative FNSB was observed for the fluorinated labels when compared to **11** (which was essentially unchanged) when Tween-20 was used as the wash detergent. To determine whether specific fluorous interactions between SPFO and the fluorinated acridinium esters could be used to augment the wash efficacy of Tween-20, a third wash protocol using a mixture of SPFO and Tween-20 was evaluated (Table 5) but we observed no further reduction in the FNSB values of the fluorinated acridinium esters. The dominant interaction between the conjugates of the fluorinated acridinium esters and the PMPs appears to be largely hydrophobic in nature and specific fluorous interactions between these labels and SPFO are too weak to overcome this interaction.

Conclusions

In the current study we have described the synthesis of new acridinium esters with fluorous tags and have investigated their light emission in the presence of cationic micelles of CTAC, anionic micelles of the perfluorinated surfactant SPFO as well as mixed micelles these two surfactants. We have also compared the chemiluminescence stability and non-specific binding of these labels to that of a structurally analogous but non-fluorinated acridinium ester. Our main findings and observations can be summarized in the following points:

1. Fluorous tags in acridinium esters, installed at C-2 ether linkages of the acridinium ring, have either a minimal or only a small impact on their chemiluminescence emission spectra when compared to an analogously C-2 alkoxy substituted, non-fluorinated acridinium ester.

2. Fluorinated acridinium esters partition equally well into micelles of the cationic surfactant CTAC as a non-fluorinated acridinium ester. Fast light emission and similar quantum yields (comparable to a non-fluorinated acridinium ester) are observed for these new labels. Thus, fluorous tags in acridinium esters do not lead to solubilization of the labels into a less polar region of CTAC micelles as reported for SPFO in CTAC micelles. Because charged reactive ions and charged reaction intermediates are involved in the chemiluminescence reaction pathway of acridinium esters, these results are not entirely unexpected. The chemiluminescence reaction most likely proceeds at the Stern layer of the micelle.

3. Mixed micelles of CTAC : SPFO at low mole fractions of SPFO behave like less polar micelles of cationic surfactants with large head groups such as cetyltripropylammonium chloride based on the observed enhancement in light yields when compared to CTAC micelles.[1d] Fluorous interactions between fluorinated acridinium esters and SPFO in the mixed micelles do not lead to greater enhancement of light yields for the same reason noted in 2. Evidence for fluorous interactions between the fluorinated acridinium esters and SPFO was noted in pure anionic SPFO micelles where inhibition of emission kinetics and depressed light yield was observed.

4. Chemiluminescence stability of fluorinated acridinium esters at 37 °C and neutral pH are either comparable to or better than the stability of a non-fluorinated acridinium ester.

5. Fluorinated acridinium esters are lipophilic and require a detergent wash to reduce their non-specific binding to paramagnetic microparticles.

From the current study, we can identify two fluorinated acridinium esters, compound **5a** (F9AE) and **5b** (F13AE) as improvements over the non-fluorinated acridinium ester **11** owing to their higher light yield (Table 1), better chemiluminescence stability (Fig. 7) and equivalent non-specific binding (Table 5).

Experimental

General

Chemicals were purchased from Sigma-Aldrich (Milwaukee, Wisconsin, USA) unless indicated otherwise. The ionic liquids [BMIM][PF_6] and [BMIM][BF_4] were dried under high vacuum over P_2O_5 prior to use. Sodium perfluorooctanoate (SPFO) was purchased from Alfa-Aesar.

All final acridinium esters, intermediates and reaction mixtures were analyzed and/or purified by HPLC using a Beckman-Coulter HPLC system. For analytical HPLC, a Phenomenex, Kinetex, XB-C_{18}, 2.6 micron, 4.6 × 50 mm column was used with MeCN–water (each with 0.05% trifluoroacetic acid, TFA) as the solvents at a flow rate of 1 mL min^{-1} and UV detection at 260 nm. Preparative HPLC was performed using a Phenomenex, *Luna* C_{18}, 5 micron, 250 × 30 mm column at a flow rate of 16–20 mL min^{-1} and UV detection at 260 nm. Flash chromatography was performed using an 'Autoflash' system from TELEDYNE ISCO. MALDI-TOF (Matrix-Assisted Laser Desorption Ionization-Time of Flight) mass spectroscopy was performed using a VOYAGER DE Biospectrometry Workstation from ABI. This is a bench top instrument operating in the linear mode with a 1.2 meter ion path length, flight tube. Spectra were acquired in positive ion mode. For small molecules, α-cyano-4-hydroxycinnamic acid was used as the matrix and spectra were acquired with an accelerating voltage of 20 000 volts and a delay time of 100 ns. For protein conjugates, sinapinic acid was used as the matrix and spectra were acquired with an accelerating voltage of 25 000 volts and a delay time of 85 ns.

For HRMS (High Resolution Mass Spectra), samples were dissolved in HPLC-grade methanol and analyzed by direct-flow injection (injection volume = 5 μL) ElectroSpray Ionization (ESI) on a Waters Qtof API US instrument in the positive ion mode. Optimized conditions were as follows: capillary = 3000 kV, cone = 35, source temperature = 120 °C, desolvation temperature = 350 °C.

NMR spectra (proton and fluorine) were recorded on a Varian 500 MHz spectrometer. To suppress or minimize pseudobase formation (Fig. 2, **II** to **1** conversion), spectra of the fluorinated acridinium esters and intermediates were acquired in an acidic solvent, namely deuterated acetic acid so that two forms of the compounds were not present during spectral analysis. Significant line broadening was observed in deuterated trifluoroacetic acid and therefore this acidic solvent was unsuitable for proton NMR analysis of the fluorinated acridinium esters. Because of limited solubility of the fluorinated acridinium compounds in deuterated acetic acid, carbon NMR spectra could not be acquired.

Chemiluminescence measurements were carried out using a Berthold Technologies' AutoLumat Plus LB 953 luminometer. Emission spectra were recorded in >90% aqueous media using a PR-740 spectroradiometer (camera) on loan from Photo Research Inc. Bandwidth slit: 2 nm; aperture: 2 degrees; exposure time: 5000 ms.

Synthesis of acridinium esters (Fig. 4–6, and Fig. S1–S24 ESI†)

Compound 2a. Compound **1** (100 mg, 0.249 mmol) was dissolved in acetonitrile (15 mL) and potassium carbonate (38 mg, 0.274 mmol) was added followed by 1*H*,1*H*,2*H*,2*H*-perfluorohexyl triflate (197 mg, 0.498 mmol) and the reaction was stirred at room temperature for 16 hours. The reaction mixture was concentrated under reduced pressure. The residue was extracted with dichloromethane (70 mL) and subsequently washed with water (30 mL). The organic layer was dried over anhydrous sodium sulfate and concentrated under reduced pressure. The crude product was purified by flash chromatography on silica (40 g column) using a 30 minute gradient of 0 → 100% B (solvent A: hexanes; solvent B: hexanes–ethyl acetate, 1 : 1). Yield = 145 mg (90%). δ_H (500 MHz, $CDCl_3$) 2.47 (s, 6H), 2.75 (m, 2H), 3.95 (s, 3H), 4.42 (t, 2H, J = 6.7 Hz), 7.54 (dd, 1H, J = 9.4 Hz, 2.6 Hz), 7.61 (d, 1H, J = 2.6 Hz), 7.63–7.72 (m, 1H), 7.76–7.86 (m, 1H), 7.92 (s, 2H), 8.24 (d, 1H, J = 9.4 Hz), 8.31 (dd, 1 H, J = 8.7 Hz, 1.1 Hz), 8.43 (dd, 1H, J = 8.8 Hz, 1.1 Hz). δ_F (470 MHz, $CDCl_3$) −80.99 (t, 3F, J = 9.6 Hz), −113.46 (m, 2F), −124.44 (m, 2F), −125.93 (m, 2F). MALDI-TOF MS m/z 648.2 $(M + H)^+$; HRMS m/z 648.1423 $(M + H)^+$ (648.1433 calculated).

Compounds **2b** and **2c** were synthesized similarly.

Compound 2b. Yield = 80 mg (86%). δ_H (500 MHz, $CDCl_3$) 2.47 (s, 6H), 2.75 (m 2H), 3.95 (s, 3H), 4.42 (t, 2H, J = 6.7 Hz), 7.53 (dd, 1H, J = 9.5 Hz, 2.6 Hz), 7.61 (d, 1H, J = 2.6 Hz), 7.68 (m, 1H), 7.82 (m, 1H), 7.92 (s, 2H), 8.24 (d, 1H, J = 9.5 Hz), 8.31 (m, 1H), 8.43 (m, 1H). δ_F (470 MHz, $CDCl_3$) −80.76 (t, 3F, J = 11.1 Hz), −113.26 (m, 2F), −121.82 (m, 2F), −122.84 (m, 2F), −123.51 (m, 2F), −126.12 (m, 2F). MALDI-TOF MS m/z 748.4 $(M + H)^+$; HRMS m/z 748.1363 $(M + H)^+$ (748.1369 calculated).

Compound 2c. Yield = 95 mg (90%). δ_H (500 MHz, $CDCl_3$) 2.47 (s, 6H), 2.75 (m, 2H), 3.94 (s, 3H), 4.42 (t, 2H, J = 6.7 Hz), 7.53 (dd, 1H, J = 9.4 Hz, 2.7 Hz), 7.61 (d, 1H, J = 2.6 Hz), 7.68 (m, 1H), 7.81 (m, 1H), 7.92 (s, 2H), 8.24 (d, 1H, J = 9.5 Hz), 8.30 (br d, 1H, J = 8.5 Hz), 8.43 (br d, 1H, J = 8.4 Hz). δ_F (470 MHz, $CDCl_3$) −80.73 (t, 3F, J = 9.9 Hz), −113.24 (m, 2F), −121.60 (m, 2F), −121.88 (m, 4F), −122.69 (m, 2F), −123.46 (m, 2F), −126.09 (m, 2F). MALDI-TOF MS m/z 848.1 $(M + H)^+$; HRMS m/z 848.1290 $(M + H)^+$ (848.1305 calculated).

Compound 3a. Compound **2a** (100 mg, 0.154 mmol) in [BMIM][PF_6] (1 mL) and 2,6-di-*tert*-butylpyridine (0.256 mL, 1.158 mmol) was treated with 1,3-propane sultone (283 mg, 2.317 mmol). The mixture was heated at 155 °C in a sealed vial for 16 hours and then cooled to room temperature. The reaction mixture was diluted with ethyl acetate (1 mL) and purified by flash chromatography on silica (40 g column) using pure ethyl acetate as eluent to remove unreacted starting material and base followed by 40% ethyl acetate in methanol to elute product. Yield = 99 mg (83% yield). This *N*-sulfopropyl acridinium methyl ester was carried as such to the next step. Thus, 89 mg of the acridinium methyl ester was refluxed in a mixture of 2 N HCl–acetonitrile (1 : 1) for 16 hours. The reaction mixture was cooled to room temperature and product **3a** was purified by preparative HPLC using a 30 minute gradient of

10 → 90% MeCN–water (each with 0.05% TFA). The HPLC fractions were concentrated under reduced pressure. Yield = 84 mg (80%). δ_H (500 MHz, CD_3COOD) 2.69 (s, 6H), 2.86–2.96 (m, 2 H), 2.99–3.13 (m, 2H), 3.63 (m, 2H), 4.80 (t, 2H, J = 6.2 Hz), 6.02 (m, 2H), 7.98 (d, 1H, J = 2.7 Hz), 8.15 (m, 2H), 8.30 (dd, 1H, J = 8.8 Hz, 6.7 Hz), 8.45 (dd, 1H, J = 10.0 Hz, 2.8 Hz), 8.66 (m, 1H), 8.78 (dd, 1H, J = 8.8 Hz, 1.3 Hz), 9.15 (d, 1H, J = 9.4 Hz), 9.22 (d, 1H, J = 10.1 Hz). δ_F (470 MHz, CD_3COOD) −81.95 (t, 3F, J = 9.8 Hz), −113.88 (m, 2F), −124.93 (m, 2F), −126.57 (m, 2F). MALDI-TOF MS m/z 756.2 $(M + H)^+$; HRMS m/z $(M + H)^+$ 756.1304 (756.1314 calculated).

Compounds **3b** and **3c** were synthesized similarly.

Compound 3b. Yield = 38 mg (67%). δ_H (500 MHz, CD_3COOD) 2.67 (s, 6H), 2.80–2.93 (m, 2H), 2.98–3.10 (m, 2H), 3.57–3.64 (m, 2H), 4.78 (t, 2H, J = 6.2 Hz), 6.00 (t, 2H, J = 9.5 Hz), 7.97 (d, 1H, J = 2.8 Hz), 8.13 (s, 2 H), 8.28 (dd, 1H, J = 8.8 Hz, 6.7 Hz), 8.44 (m, 1H), 8.64 (m, 1H), 8.76 (dd, 1H, J = 8.8 Hz, 1.3 Hz), 9.13 (d, 1H, J = 9.4 Hz), 9.21 (d, 1H, J = 10.1 Hz). δ_F (470 MHz, CD_3COOD) −81.70 (t, 3F, J = 10.1 Hz), −113.60 (m, 2F), −122.33 (m, 2F), −123.37 (m, 2F), −123.92 (m, 2F), −126.70 (m, 2F). MALDI-TOF MS m/z 856.2 $(M + H)^+$; HRMS m/z 856.1249 $(M + H)^+$ (856.1250 calculated).

Compound 3c. Yield = 20 mg (36%). δ_H (500 MHz, CD_3COOD) 2.67 (s, 6H), 2.83–2.94 (m, 2H), 2.98–3.13 (m, 2H), 3.60 (m, 2H), 4.78 (t, 2H, J = 6.2 Hz), 6.00 (m, 2H), 7.96 (d, 1H, J = 2.7 Hz), 8.13 (s, 2H), 8.27 (dd, 1H, J = 8.8 Hz, 6.7 Hz), 8.43 (dd, 1H, J = 10.0 Hz, 2.7 Hz), 8.63 (m, 1H), 8.76 (dd, 1H, J = 8.8 Hz, 1.3 Hz), 9.13 (d, 1H, J = 9.4 Hz), 9.20 (d, 1H, J = 10.1 Hz). δ_F (470 MHz, CD_3COOD) −81.67 (t, 3F, J = 10.0 Hz), −113.57 (m, 2F), −121.11 (m, 2F), −122.36 (m, 4F), −123.22 (m, 2F), −123.85 (m, 2F), −126.68 (m, 2F). MALDI-TOF MS m/z 956.1 $(M + H)^+$; HRMS m/z 956.1197 $(M + H)^+$ (956.1186 calculated).

Compound 4a. Compound **3a** (60 mg, 0.079 mmol) was suspended in DMF (3 mL) and diisopropylethylamine (0.021 mL, 0.119 mmol) and *N*,*N*,*N*′,*N*′-tetramethyl-*O*-(*N*-succinimidyl)-uronium tetrafluoroborate (TSTU, 29 mg, 0.095 mmol) were added. The reaction was stirred at room temperature for 1 hour and was then added drop wise to a stirred solution of **iv** (170 mg, 0.397 mmol, HBr salt) dissolved in 0.5 M sodium bicarbonate (3 mL) cooled in an ice bath. After 16 hours, the reaction mixture was purified by preparative HPLC as described earlier using a 40 minute gradient 10 → 40% MeCN–water (each with 0.05% TFA). The HPLC fractions containing product **4a** were concentrated under reduced pressure. Yield = 60 mg (75%). δ_H (500 MHz, CD_3COOD) 2.28–2.39 (m, 2H), 2.39–2.52 (m, 4H), 2.55 (s, 6H), 2.78–2.86 (m, 2H), 2.96–3.10 (m, 2H), 3.21 (m, 2H), 3.27 (s, 3H), 3.40 (t, 2H, J = 7.2 Hz), 3.56 (m, 2H), 3.59–3.72 (m, 4H), 3.72–3.83 (m, 4H), 4.70 (t, 2H, J = 6.1 Hz), 5.92 (m, 2H), 7.76 (d, 1H, J = 2.7 Hz), 7.91 (s, 2H), 8.23 (dd, 1H, J = 8.8 Hz, 6.7 Hz), 8.39 (dd, 1H, J = 10.0 Hz, 2.7 Hz), 8.59 (m, 2H), 9.09 (d, 1H, J = 9.8 Hz), 9.15 (d, 1H, J = 10.0 Hz); δ_F (470 MHz, CD_3COOD) −81.92 (t, 3F, J = 9.9 Hz), −113.91 (m, 2F), −124.94 (m, 2F), −126.54 (m, 2F). MALDI-TOF MS m/z 1005.4 $(M + H)^+$; HRMS m/z 1005.2835 $(M + H)^+$ (1005.2825 calculated).

Compounds **4b** and **4c** were synthesized similarly.

Compound 4b. Yield = 23 mg (59%). δ_H (500 MHz, CD_3COOD) 2.32–2.42 (m, 2H), 2.42–2.52 (m, 4H), 2.53 (s, 6H), 2.73–2.88 (m, 2H), 2.97–3.15 (m, 2H), 3.23 (t, 2H, J = 6.6 Hz), 3.29 (s, 3H), 3.42 (t, 2H, J = 7.1 Hz), 3.56 (m, 2H), 3.61–3.74 (m, 4H), 3.74–3.86 (m, 4H), 4.69 (t, 2H, J = 6.0 Hz), 5.92 (m, 2H), 7.71 (m, 1H), 7.91 (s, 2H), 8.23 (m, 1H), 8.41 (dd, 1H, J = 10.0 Hz, 2.6 Hz), 8.52 (d, 1H, J = 8.7 Hz), 8.62 (m, 1H), 9.10 (d, 1H, J = 9.5), 9.16 (d, 1H, J = 10.1 Hz). δ_F (470 MHz, CD_3COOD) −81.71 (t, 3F, J = 10.1 Hz), −113.78 (m, 2F), −122.36 (m, 2F), −123.39 (m, 2F), −124.02 (m, 2F), −126.75 (m, 2F). MALDI-TOF MS m/z 1105.3 $(M + H)^+$; HRMS m/z 1105.2769 $(M + H)^+$ (1105.2761 calculated).

Compound 4c. Yield = 8 mg (52%). δ_H (500 MHz, CD_3COOD) 2.31–2.39 (m, 2H), 2.39–2.53 (m, 4H), 2.63 (s, 6H), 2.78–2.95 (m, 2H), 2.97–3.15 (m, 2H), 3.24 (m, 2H), 3.26 (s, 3H), 3.38 (t, 2H, J = 7.1 Hz), 3.55–3.71 (m, 6H), 3.71–3.85 (m, 4H), 4.75 (t, 2H, J = 6.1 Hz), 5.98 (m, 2H), 7.89 (d, 1H, J = 2.8 Hz), 7.94 (s, 2H), 8.27 (m, 1H), 8.42 (dd, 1H, J = 9.9 Hz, 2.7 Hz), 8.63 (m, 1H), 8.70 (d, 1H, J = 8.7 Hz), 9.12 (d, 1H, J = 9.5 Hz), 9.19 (d, 1H, J = 10.1 Hz). δ_F (470 MHz, CD_3COOD) −81.67 (t, 3F, J = 10.1 Hz), −113.75 (m, 2F), −122.09 (m, 2F), −122.38 (m, 4F), −123.24 (m, 2F), −123.93 (m, 2F), −126.67 (m, 2F). MALDI-TOF MS m/z 1205.4 $(M + H)^+$; HRMS m/z 1205.2703 $(M + H)^+$ (1205.2697 calculated).

Compound 5a. Compound **4a** (30 mg, 0.030 mmol) was dissolved in methanol (2 mL) and diisopropylethylamine (DIPEA, 0.026 mL, 0.149 mmol) and glutaric anhydride (17.0 mg, 0.149 mmol) were added. The reaction was stirred at room temperature and monitored by analytical HPLC which showed 98% conversion. The reaction mixture was concentrated under reduced pressure. The residue was dissolved in DMF (2 mL) and DIPEA (0.104 mL, 0.597 mmol) and TSTU (180 mg, 0.597 mmol) were added. The reaction was stirred at room temperature and monitored by analytical HPLC which showed complete conversion to the *N*-hydroxysuccinimide ester. The product **5a** was purified by preparative HPLC as described earlier using a 40 minute gradient of 10 → 60% MeCN–water (each with 0.05% TFA). The HPLC fractions containing product **5a** were frozen at −80 °C and lyophilized to dryness. Yield = 28 mg (76%). δ_H (500 MHz, CD_3COOD) 2.28–2.36 (m, 2H), 2.36–2.47 (m, 2H), 2.51–2.64 (m, 8H), 2.81 (m, 6H), 2.88–3.12 (m, 8H), 3.17–3.28 (m, 5H), 3.44–3.65 (m, 8H), 3.67–3.77 (m, 4H), 4.72 (t, 2H, J = 6.0 Hz), 5.95 (m, 2H), 7.81 (d, 1H, J = 2.8 Hz), 7.93 (s, 2H), 8.25 (dd, 1H, J = 8.7 Hz, 6.8 Hz), 8.41 (dd, 1H, J = 10.0 Hz, 2.7 Hz), 8.62 (m, 2H), 9.12 (d, 1H, J = 9.6 Hz), 9.18 (d, 1H, J = 10.1 Hz). δ_F (470 MHz, CD_3COOD) −81.90 (m, 3F), −113.88 (m, 2F), −124.92 (m, 2F), −126.53 (m, 2F). MALDI-TOF MS m/z 1216.4 $(M + H)^+$; HRMS m/z 1216.3448 $(M + H)^+$ (1216.3305 calculated).

Compounds **5b** and **5c** were synthesized similarly.

Compound 5b. Yield = 8 mg (45%). δ_H (500 MHz, CD_3COOD) 2.28–2.37 (m, 2H), 2.37–2.47 (m, 2H), 2.47–2.64 (m, 8H), 2.76–2.87 (m, 6H), 2.95–3.12 (m, 8H), 3.15–3.25 (m, 5H), 3.46–3.65 (m, 8H), 3.68–3.78 (m, 4H), 4.71 (t, 2H, J = 6.1 Hz), 5.93 (m, 2H), 7.78 (d, 1H, J = 2.8 Hz), 7.92 (s, 2H), 8.24 (dd, 1H,

J = 8.8 Hz, 6.7 Hz), 8.41 (dd, 1H, J = 9.9 Hz, 2.7 Hz), 8.55–8.67 (m, 2H), 9.11 (d, 1H, J = 9.5 Hz), 9.17 (d, 1H, J = 10.1 Hz). δ_F (470 MHz, CD_3COOD) −81.69 (t, 3F, J = 10.0 Hz), −113.69 (m, 2F), −122.30 (m, 2F), −123.36 (m, 2 F), −123.96 (m, 2F), −126.69 (m, 2F). MALDI-TOF MS m/z 1316.8 $(M + H)^+$; HRMS m/z 1316.3292 $(M + H)^+$ (1316.3242 calculated).

Compound 5c. Yield = 2 mg (17%). δ_H (500 MHz, CD_3COOD) 2.27–2.36 (m, 2H), 2.36–2.46 (m, 2H), 2.46–2.57 (m, 2H), 2.62 (s, 6H), 2.71–2.90 (m, 6H), 2.93–3.13 (m, 8H), 3.17–3.27 (m, 5H), 3.46–3.66 (m, 8H), 3.67–3.77 (m, 4H), 4.74 (t, 2H, J = 6.1 Hz), 5.96 (m, 2H), 7.86 (d, 1H, J = 2.8 Hz), 7.93 (s, 2H), 8.25 (m, 1 H), 8.41 (dd, 1H, J = 10.0 Hz, 2.7), 8.62 (m, 1H), 8.67 (m, 1H), 9.11 (d, 1H, J = 9.4 Hz), 9.18 (d, 1H, J = 10.1 Hz). δ_F (470 MHz, CD_3COOD) −81.66 (t, 3F, J = 10.0 Hz), −113.69 (m, 2F), −122.06 (m, 2F), −122.36 (m, 4F), −123.21 (m, 2F), −123.90 (m, 2F), −126.67 (m, 2F). MALDI-TOF MS m/z 1416.5 $(M + H)^+$; HRMS m/z 1416.3582 $(M + H)^+$ (1416.3178 calculated).

Compound 7a. Compound **6** (100 mg, 0.206 mmol) was dissolved in acetonitrile (15 mL) and 1*H*,1*H*,2*H*,2*H*-perfluorohexyl triflate (163 mg, 0.411 mmol) was added. The reaction was stirred at room temperature for 1 hour and monitored by analytical HPLC which showed 89% conversion. The crude mixture was purified by preparative HPLC as described earlier using a 30 minute gradient of 10 → 90% MeCN–water (each with 0.05% TFA). The HPLC fractions containing product **7a** were concentrated under reduced pressure. Yield = 163 mg (94%). δ_H (500 MHz, CD_3CN) 2.31 (m, 2H), 2.49 (s, 6H), 2.72–2.86 (m, 2H), 3.11 (s, 6H), 3.55 (m, 2H), 3.65 (m, 2H), 3.90 (s, 3H), 4.26 (t, 2 H, J = 5.6 Hz), 7.63 (m, 2H), 7.76–7.86 (m, 1H), 7.88–7.96 (m, 3H), 8.31 (d, 1H, J = 9.4 Hz), 8.34 (d, 1H, J = 8.7 Hz), 8.45 (d, 1H, J = 8.7 Hz); δ_F (470 MHz, CD_3CN) −81.80 (t, 3F, J = 9.7 Hz), −114.10 (m, 2F), −124.35 (m, 2F), −126.52 (m, 2F). MALDI-TOF MS m/z 733.3 $(M)^+$; HRMS m/z 733.2347 $(M)^+$ (733.2324 calculated).

Compounds **7b** and **7c** were synthesized similarly.

Compound 7b. Yield = 25 mg (63%). δ_H (500 MHz, CD_3CN) 2.31 (m, 2H), 2.49 (s, 6H), 2.72–2.86 (m, 2H), 3.11 (s, 6H), 3.55 (m, 2H), 3.65 (m, 2H), 3.90 (s, 3H), 4.26 (t, 2H, J = 5.6 Hz), 7.59–7.64 (m, 2H), 7.79 (m, 1H), 7.90 (m, 1H), 7.92 (s, 2H), 8.28 (m, 1H), 8.31 (m, 1H), 8.45 (m, 1H); δ_F (470 MHz, CD_3CN) −81.54 (t, 3F, J = 9.8 Hz), −113.84 (m, 2 F), −122.31 (m, 2F), −123.37 (m, 4F), −126.62 (m, 2F). MALDI-TOF MS m/z 833.3 $(M)^+$; HRMS m/z 833.2259 $(M)^+$ (833.2260 calculated).

Compound 7c. Yield = 81 mg (73%). δ_H (500 MHz, CD_3CN) 2.31 (m, 2H), 2.48 (s, 6H), 2.70–2.86 (m, 2H), 3.11 (s, 6H), 3.55 (m, 2H), 3.65 (m, 2H), 3.90 (s, 3H), 4.25 (t, 2H, J = 5.7 Hz), 7.57–7.63 (m, 2H), 7.77 (m, 1H), 7.88 (m, 1H), 7.92 (m, 2H), 8.25 (m, 1H), 8.28 (m, 1H), 8.44 (m, 1H); δ_F (470 MHz, CD_3CN) −81.52 (m, 3F), −113.86 (m, 2F), −122.12 (m, 2F), −122.32 (m, 4F), −123.15 (m, 2F), −123.38 (m, 2F), −126.58 (m, 2F). MALDI-TOF MS m/z 933.4 $(M)^+$; HRMS m/z 933.2164 $(M)^+$ (933.2196 calculated).

Compound 8a. Compound **7a** (100 mg, 0.118 mmol), 2,6-di-*tert*-butylpyridine (0.196 mL, 0.886 mmol) and 1,3-propane sultone (216 mg, 1.772 mmol) were added to [BMIM][BF_4] (1 mL). The reaction was heated at 155 °C in a sealed vial for 16 hours and then cooled to room temperature. The reaction mixture was then transferred into a flask with acetonitrile (5 mL) and 2 N HCl (20 mL) was added. The reaction was refluxed for 16 h and then cooled to room temperature. The crude reaction mixture was purified by preparative HPLC as described earlier using a 40 minute gradient of 10 → 70% MeCN–water (each with 0.05% TFA). The HPLC fractions contain product **8a** were concentrated under reduced pressure. Yield = 119 mg (quantitative). δ_H (500 MHz, CD_3COOD) 2.62 (s, 6H), 2.64–2.73 (m, 2H), 2.77–2.88 (m, 2H), 2.99–3.15 (m, 2H), 3.47 (s, 6H), 3.55 (t, 2H, J = 6.2 Hz), 3.88–4.06 (m, 4H), 4.56 (t, 2H, J = 5.6 Hz), 5.93 (m, 2H), 7.84 (d, 1H, J = 2.6 Hz), 8.08 (s, 2H), 8.23 (dd, 1H, J = 8.8 Hz, 6.7 Hz), 8.35 (m, 1H), 8.57 (m, 1H), 8.70 (d, 1H, J = 8.7 Hz), 9.04 (d, 1H, J = 9.4 Hz), 9.13 (d, 1H, J = 9.9 Hz); δ_F (470 MHz, CD_3COOD) −81.95 (t, 3F, J = 9.8 Hz), −114.10 (m, 2F), −124.33 (m, 2F), −126.64 (m, 2F). MALDI-TOF MS m/z 841.4 $(M)^+$; HRMS m/z 841.2216 $(M)^+$ (841.2205 calculated).

Compounds **8b** and **8c** were synthesized similarly.

Compound 8b. Yield = 35 mg (63%). δ_H (500 MHz, CD_3COOD) 2.66 (s, 6H), 2.67–2.76 (m, 2H), 2.81–2.92 (m, 2H), 3.00–3.17 (m, 2H), 3.48 (s, 6H), 3.59 (m, 2H), 3.93–4.05 (m, 4H), 4.58 (t, 2H, J = 5.7 Hz), 5.98 (m, 2H), 7.88 (d, 1H, J = 2.7 Hz), 8.12 (s, 2H), 8.26 (dd, 1H, J = 8.8 Hz, 6.8 Hz), 8.38 (dd, 1H, J = 10.0 Hz, 2.7 Hz), 8.61 (m, 1H), 8.75 (dd, 1H, J = 8.7 Hz, 1.3 Hz), 9.08 (d, 1H, J = 9.5 Hz), 9.19 (d, 1H, J = 10.1 Hz); δ_F (470 MHz, CD_3COOD) −81.95 (m, 3F), −113.96 (m, 2F), −122.43 (m, 2F), −123.44 (m, 4F), −126.75 (m, 2F). MALDI-TOF MS m/z 941.4 $(M)^+$; HRMS m/z 941.2151 $(M)^+$ (941.2141 calculated).

Compound 8c. Yield = 40 mg (72%). δ_H (500 MHz, CD_3COOD) 2.67 (s, 6H), 2.69–2.78 (m, 2H), 2.80–2.92 (m, 2H), 3.00–3.20 (m, 2H), 3.43–3.70 (m, 8H), 3.92–4.20 (m, 4 H), 4.62 (m, 2H), 5.98 (m, 2H), 7.88 (m, 1H), 8.12 (s, 2H), 8.26 (m, 1H), 8.40 (m, 1H), 8.61 (m, 1H), 8.75 (d, 1H, J = 8.6 Hz), 9.09 (d, 1H, J = 9.3 Hz), 9.19 (m, 1H); δ_F (470 MHz, CD_3COOD) −81.67 (t, 3F, J = 10.1 Hz), −113.79 (m, 2F), −122.12 (m, 2F), −122.36 (m, 4 F), −123.22 (m, 4F), −126.69 (m, 2F). MALDI-TOF MS m/z 1041.2 $(M)^+$; HRMS m/z 1041.2089 $(M)^+$ (1041.2077 calculated).

Compound 9a. Compound **8a** (54 mg, 0.062 mmol) dissolved in DMF (2 mL) was treated with DIPEA (0.016 mL, 0.092 mmol) and TSTU (20 mg, 0.068 mmol). The reaction was stirred at room temperature for 30 minutes and then this solution was added drop wise to an ice cold, stirred solution of **iv** (133 mg, 0.31 mmol, HBr salt) dissolved in 0.5 M sodium bicarbonate (2 mL). The reaction was stirred at 0 °C for 2 hours. The crude product was purified by a preparative HPLC as described earlier using a 40 minute gradient of 10 → 60 MeCN–water (each with 0.05% TFA). The HPLC fractions containing product **9a** were concentrated under reduced pressure. Yield = 38 mg (55%). δ_H (500 MHz, CD_3COOD) 2.27–2.38 (m, 2H), 2.47 (m, 4H), 2.58 (s, 6H), 2.70 (m, 2H), 2.82 (m, 2H), 2.99–3.24 (m, 4H), 3.26 (s, 3H), 3.38 (m, 2H), 3.48 (s, 6H), 3.52–3.85 (m, 10H), 3.98 (m, 4H), 4.49 (m, 2H), 5.93 (m, 2H), 7.73 (d, 1H, J = 2.7 Hz), 7.88 (s, 2H), 8.25 (m, 1H), 8.33

(dd, 1H, J = 10.0 Hz, 2.7 Hz), 8.58 (m, 1H), 8.70 (m, 1H), 9.04 (d, 1H, J = 9.4 Hz), 9.14 (d, 1H, J = 10.1 Hz); δ_F (470 MHz, CD_3COOD) −81.93 (m, 3F), −114.06 (m, 2F), −124.31 (m, 2F), −126.61 (m, 2F). MALDI-TOF MS m/z 1090.5 $(M)^+$; HRMS m/z 1090.3828 $(M)^+$ (1090.3716 calculated).

Compounds **9b** and **9c** were synthesized similarly.

Compound 9b. Yield = 20 mg (65%). δ_H (500 MHz, CD_3COOD) 2.27–2.38 (m, 2H), 2.49 (m, 4H), 2.63 (s, 6H), 2.73 (m, 2H), 2.85 (m, 2H), 3.04–3.13 (m, 2H), 3.17 (m, 2H), 3.27 (s, 3H), 3.37 (m, 2H), 3.49 (s, 6H), 3.55–3.90 (m, 10H), 3.96–4.05 (m, 4H), 4.52 (m, 2 H), 5.97 (m, 2H), 7.78 (d, 1H, J = 2.7 Hz), 7.92 (s, 2H), 8.28 (dd, 1H, J = 8.7 Hz, 6.7 Hz), 8.35 (dd, 1H, J = 10.0 Hz, 2.7 Hz), 8.61 (m, 1H), 8.78 (d, 1H, J = 8.7 Hz), 9.08 (d, 1H, J = 9.4 Hz), 9.19 (d, 1H, J = 10.1 Hz); δ_F (470 MHz, CD_3COOD) −81.69 (m, 3F), −113.90 (m, 2F), −122.39 (m, 2F), −123.39 (m, 4F), −126.73 (m, 2F). MALDI-TOF MS m/z 1191.5 $(M + H)^+$; HRMS m/z 1190.3691 $(M)^+$ (1190.3652 calculated).

Compound 9c. Yield = 4 mg (14%). δ_H (500 MHz, CD_3COOD) 2.27–2.38 (m, 2H), 2.48 (m, 4H), 2.62 (s, 6H), 2.72 (m, 2H), 2.85 (m, 2H), 3.02–3.21 (m, 4H), 3.27 (s, 3H), 3.38 (m, 2H), 3.49 (s, 6H), 3.55–3.92 (m, 10H), 3.96–4.08 (m, 4H), 4.51 (m, 2H), 5.97 (m, 2H), 7.77 (d, 1H, J = 2.7 Hz), 7.91 (s, 2H), 8.28 (m, 1H), 8.35 (m, 1H), 8.61 (m, 1H), 8.77 (d, 1H, J = 8.6 Hz), 9.07 (d, 1H, J = 9.4 Hz), 9.19 (d, 1H, J = 10.1 Hz); δ_F (470 MHz, CD_3COOD) −81.67 (t, 3F, J = 10.1 Hz), −113.83 (m, 2F), −122.13 (m, 2F), −122.35 (m, 4F), −123.25 (m, 4F), −126.68 (m, 2F). MALDI-TOF MS m/z 1290.5 $(M)^+$; HRMS m/z 1290.3627 $(M)^+$ (1290.3588 calculated).

Compound 10a. Compound **9a** (20 mg, 0.018 mmol) was dissolved in methanol (2 mL) and DIPEA (0.031 mL, 0.178 mmol) and glutaric anhydride (10 mg, 0.089 mmol) were added. The reaction was stirred at room temperature for 1 hour and was then concentrated under reduced pressure. The residue was dissolved in DMF (2 mL) and DIPEA (0.062 mL, 0.355 mmol) and TSTU (107 mg, 0.355 mmol) were added. The reaction was stirred at room temperature for 1 hour. The crude reaction mixture was purified by preparative HPLC as described earlier using a 40 minute gradient of 10 → 60% MeCN–water (each with 0.05% TFA). The HPLC fractions containing product **10a** were frozen at −80 °C and lyophilized to dryness. Yield = 22 mg (93%). δ_H (500 MHz, CD_3COOD) 2.27–2.38 (m, 2H), 2.42–2.57 (m, 6H), 2.63 (s, 6H), 2.67–2.78 (m, 2H), 2.80 (m, 2H), 2.84 (m, 4H), 2.96–3.12 (m, 10H), 3.17 (m, 2H), 3.23 (s, 3H), 3.50 (s, 6H), 3.51–3.90 (m, 8H), 3.95–4.08 (m, 4H), 4.52 (m, 2H), 5.98 (m, 2H), 7.78 (d, 1H, J = 2.7 Hz), 7.93 (s, 2H), 8.29 (m, 1H), 8.36 (dd, 1H, J = 9.9 Hz, 2.7 Hz), 8.61 (m, 1H), 8.77 (m, 1H), 9.08 (d, 1H, J = 9.4 Hz), 9.19 (d, 1H, J = 10.1 Hz); δ_F (470 MHz, CD_3COOD) −81.92 (t, 3F, J = 9.9 Hz), −114.07 (m, 2F), −124.29 (m, 2F), −126.60 (m, 2F). MALDI-TOF MS m/z 1301.7 $(M)^+$; HRMS m/z 1301.4341 $(M)^+$ (1301.4191 calculated).

Compounds **10b** and **10c** were synthesized similarly.

Compound 10b. Yield = 12 mg (68%). δ_H (500 MHz, CD_3COOD) 2.27–2.35 (m, 2H), 2.42–2.57 (m, 6H), 2.60 (s, 6H), 2.67–2.78 (m, 2H), 2.78–2.94 (m, 6H), 2.95–3.12 (m, 10H), 3.17 (m, 2H), 3.23 (s, 3H), 3.49 (s, 6H), 3.51–3.90 (m, 8H), 3.95–4.08 (m, 4H), 4.51 (t, 2H, J = 5.6 Hz), 5.97 (m, 2H), 7.77 (d, 1H, J = 2.7 Hz), 7.91 (s, 2H), 8.28 (dd, 1H, J = 8.8 Hz, 6.7 Hz), 8.35 (dd, 1H, J = 10.0 Hz, 2.7 Hz), 8.61 (m, 1H), 8.76 (dd, 1H, J = 8.7 Hz, 1.4 Hz), 9.07 (d, 1H, J = 9.5 Hz), 9.18 (d, 1H, J = 10.1 Hz); δ_F (470 MHz, CD_3COOD) −81.67 (m, 3F), −113.84 (m, 2F), −122.37 (m, 2F), −123.36 (m, 4F), −126.69 (m, 2F). MALDI-TOF MS m/z 1402.9 $(M + H)^+$; HRMS m/z 1401.4303 $(M)^+$ (1401.4133 calculated).

Compound 10c. Yield = 3 mg (50%). δ_H (500 MHz, CD_3COOD) 2.26–2.34 (m, 2H), 2.42–2.61 (m, 6H), 2.63 (s, 6H), 2.67–2.74 (m, 2H), 2.78–2.90 (m, 6H), 2.95–3.12 (m, 10 H), 3.19 (m, 2H), 3.22 (s, 3H), 3.50 (s, 6H), 3.51–3.90 (m, 8H), 3.95–4.08 (m, 4H), 4.52 (m, 2H), 5.98 (m, 2H), 7.79 (d, 1H, J = 2.7 Hz), 7.91 (s, 2H), 8.28 (dd, 1H, J = 8.7 Hz, 6.7 Hz), 8.35 (dd, 1H, J = 10.0 Hz, 2.7 Hz), 8.61 (m, 1H), 8.79 (d, 1H, J = 8.5 Hz), 9.07 (d, 1H, J = 9.4 Hz), 9.19 (d, 1H, J = 10.1 Hz); δ_F (470 MHz, CD_3COOD) −81.66 (t, 3F, J = 10.1 Hz), −113.83 (m, 2F), −122.13 (m, 2F), −122.37 (m, 4F), −123.25 (m, 4F), −126.69 (m, 2F). MALDI-TOF MS m/z 1501.9 $(M)^+$; HRMS m/z 1501.4374 $(M)^+$ (1501.4069 calculated).

Acknowledgements

We thank Dr Shenliang Wang for assistance in emission spectra measurements.

References

1 (*a*) A. Natrajan, D. Sharpe and Q. Jiang, *US Pat* 6,664,043 B2, 2003; (*b*) A. Natrajan, Q. Jiang, D. Sharpe and J. Costello, *US Pat* 7,309,615 B2, 2007; (*c*) A. Natrajan, D. Sharpe, J. Costello and Q. Jiang, *Anal. Biochem.*, 2010, **406**, 204–213; (*d*) A. Natrajan, D. Sharpe and D. Wen, *Org. Biomol. Chem.*, 2011, **9**, 5092–5103; (*e*) A. Natrajan, D. Sharpe and D. Wen, *Org. Biomol. Chem.*, 2012, **10**, 1883–1895; (*f*) A. Natrajan, D. Sharpe and D. Wen, *Org. Biomol. Chem.*, 2012, **10**, 3432–3447; (*g*) A. Natrajan and D. Sharpe, *Org. Biomol. Chem.*, 2013, **11**, 1026–1039.

2 (*a*) F. McCapra, *Acc. Chem. Res.*, 1976, **9/6**, 201–208; (*b*) F. McCapra, D. Watmore, F. Sumun, A. Patel, I. Beheshti, K. Ramakrishnan and J. Branson, *J. Biolumin. Chemilumin.*, 1989, **4**, 51–58; (*c*) J. Rak, P. Skurski and J. Błażejowski, *J. Org. Chem.*, 1999, **64**, 3002–3008; (*d*) K. Krzymiński, A. Ożóg, P. Malecha, A. D. Roshal, A. Wróblewska, B. Zadykowicz and J. Błażejowski, *J. Org. Chem.*, 2011, **76**, 1072–1085.

3 (*a*) I. Weeks, I. Behesti, F. McCapra, A. K. Campbell and J. S. Woodhead, *Clin. Chem.*, 1983, **29/8**, 1474–1479; (*b*) J. W. Bunting, V. S. F. Chew, S. B. Abhyankar and Y. Goda, *Can. J. Chem.*, 1984, **62**, 351–354; (*c*) P. W. Hammond, W. A. Wiese, A. A. Waldrop III,

N. C. Nelson and L. J. Arnold Jr., *J. Biolumin. Chemilumin.*, 1991, **6**, 35–43.

4 (*a*) R. C. Chapman, E. Ostuni, L. Yan and G. M. Whitesides, *Langmuir*, 2000, **16**, 6927–6936; (*b*) R. C. Chapman, E. Ostuni, M. N. Liang, G. Meluleni, E. Kim, L. Yan, G. Pier, H. S. Warren and G. M. Whitesides, *Langmuir*, 2001, **17**, 1225–1233; (*c*) S. J. Sofia, V. Premnath and E. W. Merrill, *Macromolecules*, 1998, **31**, 5059–5070; (*d*) Y.-H. Zhao, B.-K. Zhu, L. Kong and Y.-Y. Xu, *Langmuir*, 2007, **23**, 5779–5786; (*e*) A. R. Denes, E. B. Somers, A. C. L. Wong and F. Denes, *J. Appl. Polym. Sci.*, 2001, **81**, 3425–3438; (*f*) J. Ladd, Z. Zhang, S. Chen, J. C. Hower and S. Jiang, *Biomacromolecules*, 2008, **9**, 1357–1361; (*g*) Y. Chang, S. Chen, Z. Zhang and S. Jiang, *Langmuir*, 2006, **22**, 2222–2226; (*h*) Z. Zhang, T. Chao, S. Chen and S. Jiang, *Langmuir*, 2006, **22**, 10072–10077; (*i*) W. K. Cho, B. Kong and I. S. Choi, *Langmuir*, 2007, **23**, 5678–5682; (*j*) G. Cheng, Z. Zhang, S. Chen, J. D. Bryers and S. Jiang, *Biomaterials*, 2007, **28**, 4192–4199; (*k*) H. Kitano, A. Kawasaki, H. Kawasaki and S. Morokoshi, *J. Colloid Interface Sci.*, 2005, **282**, 340–348.

5 (*a*) E. Klein, P. Kerth and L. Lebeau, *Biomaterials*, 2008, **29**, 204–214; (*b*) K. Hu, Y. Gao, W. Zhou, J. Lian, F. Li and Z. Chen, *Langmuir*, 2009, **25**, 12404–12407; (*c*) H.-Y. Hsieh, P.-C. Wang, C.-L. Wu, C.-W. Huang, C.-C. Chieng and F.-G. Tseng, *Anal. Chem.*, 2009, **81**, 7908–7916; (*d*) H.-H. Chen, W.-C. Sung, S.-S. Liang and S.-H. Chen, *Anal. Chem.*, 2010, **82**, 7804–7813; (*e*) H.-H. Chen, C.-H. Wu, M.-L. Tsai, Y.-J. Huang and S.-H. Chen, *Anal. Chem.*, 2012, **84**, 8635–8641.

6 (*a*) R. L. Nicholson, M. L. Ladlow and D. R. Spring, *Chem. Commun.*, 2007, 3906–3908; (*b*) E. H. Song and N. LB Pohl, *Future Med. Chem.*, 2009, **1**, 889–896.

7 D. P. Curran, S. Hadida and M. He, *J. Org. Chem.*, 1997, **275**, 6714–6715.

8 D. P. Curran and Z. Y. Luo, *J. Am. Chem. Soc.*, 1999, **121**, 9069–9072.

9 (*a*) T. Asakawa, T. Kitaguchi and S. Miyagishi, *J. Surfactants Deterg.*, 1998, **1**, 195–199; (*b*) K. C. Hoang and S. Mecozzi, *Langmuir*, 2004, **20**, 7347–7350.

10 *Fluorous Chemistry*, ed. I. T. Horváth, Springer-Verlag, Berlin Heidelberg, 2012.

11 *Fluorinated Surfactants and Repellents*, ed. E. Kissa, Surfactant Science Series, Marcel Dekker, Inc., 2001.

12 (*a*) Z. Yong-Xi and L. Min, *J. Surf. Sci. Technol.*, 1991, **7**, 88–91; (*b*) J. Hao, R. Lu and H. Wang, *J. Dispersion Sci. Technol.*, 1997, **18**, 379–388; (*c*) E. J. Acosta, A. Mesbah and T. Tsui, *J. Surfactants Deterg.*, 2004, **9**, 367–376; (*d*) J. L. Lopéz-Fontán, E. Blanco, J. M. Ruso, G. Prieto, P. C. Schulz and F. Sarmiento, *J. Colloid Interface Sci.*, 2007, **312**, 425–431.

13 A. Natrajan and D. Wen, *RSC Adv.*, 2013, **3**, 21398–21404.

14 T. Bříza, J. Kvíčala, O. Paleta and J. Čermák, *Tetrahedron*, 2002, **58**, 3841–3846.

15 (*a*) P. Mukerjee, K. Korematsu, M. Ōkawauchi and G. Sugihara, *J. Phys. Chem.*, 1985, **89**, 5308–5312; (*b*) S. S. Berr and R. R. M. Jones, *J. Phys. Chem.*, 1989, **93**, 2555–2558.

16 V. Peyre, *Curr. Opin. Colloid Interface Sci.*, 2009, **14**, 305–314.